

Determination of Absolute Configurations of *N*-Formyl-3,3',4,4'-tetrahydrospiro[naphthalene-1(2*H*),2'(1'*H*)-pyridine] (**2**) and *N*-Formyl-3',4'-dihydrospiro[indan-1,2'(1'*H*)-pyridine] (**3**) by Analysis of Circular Dichroism Spectra. A Case of Two Compounds with Similar Configuration But Nearly Mirror Image CD Spectra

Lena Ripa,[†] Anders Hallberg,[†] and Jan Sandström^{*,‡}

Contribution from the Department of Organic Pharmaceutical Chemistry, BMC, Uppsala University, Box 574, SE-751 23 Uppsala, Sweden, and Division of Organic Chemistry 1, Center for Chemistry and Chemical Engineering, University of Lund, Box 124, SE-221 00 Lund, Sweden

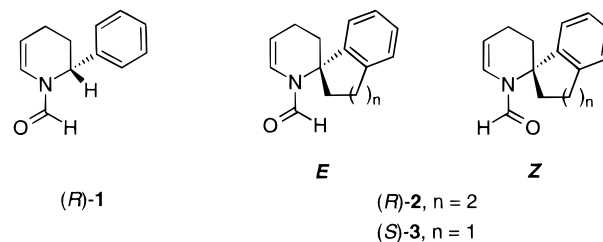
Received October 15, 1996[⊗]

Abstract: *N*-Formyl-3,3',4,4'-tetrahydrospiro[naphthalene-1(2*H*),2'(1'*H*)-pyridine] (**2**) and *N*-Formyl-3',4'-dihydrospiro[indan-1,2'(1'*H*)-pyridine] (**3**) were resolved into enantiomers, compound **3** partly and compound **2** completely, by chromatography on triacetylcellulose. The CD spectra were recorded and compared with theoretical spectra calculated by a semiempirical method, using geometries from empirical force-field calculations. In the observed CD spectra, the carbonyl $n \rightarrow \pi^*$ transitions did not give rise to visible bands, but their signs and energies were found by analysis of CD spectra in solvents of different polarity. The theoretical spectra of **2** and **3** showed complete agreement with the observed spectra in sign and qualitatively in intensity, for the five transitions observed between 190 and 280 nm, which permitted a safe assignment of the absolute configurations. The enantiomers of **2** and **3** with the aryl rings located on the same side of the tetrahydropyridine ring showed CD spectra, which were nearly mirror images, thus demonstrating the risk of deducing absolute configurations by a direct comparison of CD spectra.

Introduction

Asymmetric Heck arylations of 2,3-dihydrofurans¹ and *N*-acyl-2,3-dihydropyrroles² with (*R*)-BINAP coordinated palladium complexes as catalysts have provided fair to good enantiomeric excesses. The absolute configurations of the arylated heterocycles were determined by converting the products into derivatives with known absolute configuration.^{1a,2} In a previous study we could establish the absolute configurations of *N*-acyl-2-aryl-1,2,3,4-tetrahydropyridines³ (**1** and analogues) (Chart 1) formed after palladium catalyzed Heck reaction of aryl iodides with *N*-acyl-1,2,3,4-tetrahydropyridines by comparison of their CD spectra with spectra calculated by a semiempirical method.⁴ We⁵ have used an intramolecular Heck⁶ reaction for construction of two rigid analogues of **1**, the spiro compounds **2** and **3** (Chart 1), comprising the α -aryl piperidine fragment, common in a variety of biologically active com-

Chart 1



pounds.⁷ For an understanding of factors governing the enantioselectivity mediated by chiral ligands in the palladium catalyzed intramolecular cyclizations, knowledge of the absolute configurations of the products was essential. We now wish to report the enantiomer separation of **2** and **3** and determination of their absolute configuration by analysis of their CD spectra.

Experimental Section

Materials. The preparation of compounds **2** and **3** is reported elsewhere.⁵ The identity and purity of the compounds were verified by ¹H NMR (270 MHz), ¹³C NMR (67.8 MHz), GC-MS (EI) and by elemental analysis.

Chromatography. Instruments. Compounds **2** and **3** were resolved on two TAC columns⁸ (600 × 10 mm I.D.) in series. A Hitachi L-6000 pump set at a flow rate of 0.6 mL min⁻¹ was used as

(7) See, for example: Rubiralta, M.; Giralt, E.; Diez, A. *Piperidine. Structure, Preparation, Reactivity, and Synthetic Applications of Piperidine and its Derivatives*; Studies in Organic Chemistry 43; Elsevier: Amsterdam, 1991.

(8) TAC = swollen microcrystalline triacetylcellulose. Packed and provided by Dr Roland Isaksson, Department of Analytical Pharmaceutical Chemistry, Box 574, Uppsala University, BMC, 751 23 Uppsala, Sweden. See: Isaksson R.; Erlandsson P.; Hansson L.; Holmberg A.; Berner S. J. *Chromatogr.* **1990**, *498*, 257–280

[†] Uppsala University.

[‡] University of Lund.

[⊗] Abstract published in *Advance ACS Abstracts*, May 15, 1997.

(1) (a) Ozawa, F.; Kubo, A.; Hayashi, T. *J. Am. Chem. Soc.* **1991**, *113*, 1417–1419. (b) Ozawa, F.; Kubo, A.; Matsumoto, Y.; Hayashi, T.; Nishioka, E.; Yanagi, K.; Moriguchi, K.-i. *Organometallics* **1993**, *12*, 4188–4196.

(2) Ozawa, F.; Hayashi, T. *J. Organomet. Chem.* **1992**, *428*, 267–277.

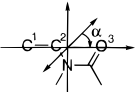
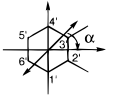
(3) Nilsson, K.; Hallberg, A. *J. Org. Chem.* **1990**, *55*, 2464–2470.

(4) Nilsson, K.; Hallberg, A.; Isaksson, R.; Sandström, J. *Acta Chem. Scand.* **1991**, *45*, 716–722.

(5) Ripa, L.; Hallberg, A. *J. Org. Chem.* **1997**, *62*, 595–602.

(6) Several successful intramolecular arylations leading to compounds with asymmetric quaternary carbon atoms have also recently been reported. (a) Cabri, W.; Candiani, I. *Acc. Chem. Res.* **1995**, *28*, 2–7. (b) de Meijere, A.; Meyer, F. E. *Angew. Chem., Int. Ed. Engl.* **1994**, *33*, 2379–2411. (c) Negishi, E.-i.; Copéret, C.; Ma, S.; Liou, S.-Y.; Liu, F. *Chem. Rev.* **1996**, *96*, 365–393. (d) Ojima, I.; Tzamarioudaki, M.; Li, Z.; Donovan, R. J. *Chem. Rev.* **1996**, *96*, 635–662. (e) Overman, L. E. *Pure Appl. Chem.* **1994**, *66*, 1423–1430. (f) Schmalz, H. -G. *Nachr. Chem. Tech. Lab.* **1994**, *42*, 270–276.

Table 1. Input Data for Theoretical Calculation of CD Spectra of **2** and **3** (The charges are in units of the protonic charge.)

chromophore	ν^a kK	μ^b D m ^c μ_B	α , deg	transition charges	static charges ^d	transition
	39.84	0.8747 ^c		0.1393 ($x, y = \pm 0.440$) ^e	$C_{ar} = -0.13$ $C_{al} = -0.20$ $H_{ar} = +0.13$ $H_{al} = +0.10$	$n \rightarrow \pi^*$
	41.40	4.65 ^b	0	O: +0.1680 ^f C-1: +0.2110 C-2: -0.3788		$\pi \rightarrow \pi^*$
	35.71	1.04	0	C-1', C-4': -0.0408 C-2', C-3': +0.0660 C-5', C-6': -0.0244		¹ L _b
	46.72	3.39	90	C-1', C-4': ± 0.2924 C-2', C-3': ± 0.5960 C-5', C-6': ± 0.4932		¹ L _a
	50.76	4.40	0	C-1', C-4': -0.0214 C-3', C-2': +0.1774 C-5', C-6': -0.1996		¹ B _b
	51.50	4.40	90	C-1', C-4': ± 0.4332 C-2', C-3': ± 0.2600 C-6', C-5': ± 0.2166		¹ B _a

^a 1 kK = 10^3 cm⁻¹. ^b Electric transition moment. ^c Magnetic transition moment in units of Bohr magnetons, directed along the C=O bond. ^d Calculated by AM1 for similar compounds. See ref 15. ^e Transition quadrupole in the xy plane of a local coordinate system with origin in the oxygen atom, the z axis along the C=O bond and the x axis in the amide plane. ^f Electric transition charges.

the solvent delivery system, and a Rheodyne 7120 valve with a 1.1 mL loop was employed to introduce the samples. Detection at 274 nm was carried out using a LCD/Milton Roy variable wavelength detector, and the chromatograms were registered with a recorder BD111 from Kipp & Zonen (Delft, The Netherlands). A Rheodyne 7000 six way valve was included in the system in order to be able to recycle part of the material after passing through the two columns. The mobile phase consisted of ethanol/water 96:4, degassed with He prior to use. The dead volume of the columns (41.4 mL) was determined by injection of 1,3,5-tri-*tert*-butylbenzene (TTB), which is supposed to be unretained by TAC.⁹ The chemical purity as well as the enantiomeric purity of the eluted compounds was checked by GLC, with the chromatograph connected to a flame ionization detector and with H₂ as carrier gas. Compound **2** was analyzed using a capillary column (10 m \times 0.32 mm), coated with 50% heptakis(6-*O-tert*-butyldimethylsilyl-2,3-di-*O*-methyl)- β -cyclodextrin in OV 1701 and compound **3** using a capillary column (20 m \times 0.32 mm), coated with 20% octakis(2,6-di-*O*-methyl-3-*O*-pentyl)- γ -cyclodextrin in OV 1701.¹⁰

N-Formyl-3,3',4,4'-tetrahydrospiro[naphthalene-1(2H),2'(1H)-pyridine] (2). Racemic **2** (49 mg) was dissolved in degassed ethanol/water (96:4, 5 mL) and filtered. Five injections were made. The first eluted band, (+)-**2**, was found to be optically pure, but the second eluted band, (-)-**2**, was reinjected. The collected fractions of each enantiomer were concentrated, taken up in 7 mL of diethyl ether, dried (K₂CO₃), and concentrated. The fractions were optically pure according to GLC. (+)-**2**, $[\alpha]_{23}^{D} +55.2$ (c 0.78, absolute ethanol), (-)-**2**, $[\alpha]_{23}^{D} -52.7$ (c 0.66, absolute ethanol).

N-Formyl-3',4'-dihydrospiro[indan-1,2'(1H)-pyridine] (3). Racemic **3** (40 mg) was dissolved in degassed ethanol/water (96:4, 3.5 mL), filtered and injected in four portions. The chromatogram showed only one broad band, but, by collecting fractions in the beginning and the end of the band, enantioenriched (-) and (+) material could be obtained. The middle fraction was recycled once. The collected fractions were concentrated, taken up in 6 mL of diethyl ether, dried (K₂CO₃), and concentrated. First eluted (-)-**3**, 37% ee, $[\alpha]_{23}^{D} -35.9$ (c 0.89, absolute ethanol), second eluted (+)-**3**, 16% ee, $[\alpha]_{23}^{D} +16.4$ (c 0.95, absolute ethanol).

Spectroscopy. Instruments. The UV spectra were recorded with a Cary Model 2290 spectrophotometer and the CD spectra with JASCO Model J-500A and 720 spectropolarimeters.

Calculations. Calculated CD Spectra. The theoretical CD spectra were obtained by a matrix method developed by Schellman and co-workers.¹¹ The method permits calculations involving both $n \rightarrow \pi^*$

and $\pi \rightarrow \pi^*$ transitions, using the one-electron¹² and the magnetic-electric ($m-\mu$) coupling¹³ mechanisms for $n \rightarrow \pi^*-\pi \rightarrow \pi^*$ couplings and the coupled oscillator mechanism¹⁴ for couplings between $\pi \rightarrow \pi^*$ transitions in different chromophores. The input in the calculations consists of transition energies, electric monopole transition charges and magnetic quadrupole transition charges, static charges, and strengths and directions of the corresponding electric and magnetic transition moments (Table 1). The derivation of the input data has recently been described in detail.¹⁶ In order to calculate the rotational strengths of the respective transitions (**R**_{*i*}) from the experimental spectra, these were simulated by gaussians, one for each transition, using a least-squares technique. The rotational strengths were obtained from eq 1, where Δ_e is the exponential half width of the Gaussian, i.e. half the width of the band where $\Delta\epsilon = \Delta\epsilon_{\max}/e$.

$$\mathbf{R} = \Delta\epsilon_{\max} \cdot \Delta_e / 2.2784 \lambda_{\max} \quad (1)$$

Empirical Force-Field Calculations. The starting structures of compounds **2** and **3** were constructed with the Macintosh molecular modeling program MacMimic¹⁷ and the energies were minimized with the Allinger MM2-91 force field.¹⁸ The nonstandard force constants used are available from the authors on request.

(10) Developed and prepared by Prof. W. A. König, Institut für Organische Chemie, Universität Hamburg, D-201 46 Hamburg, Germany.

(11) (a) Bayley, P. M.; Nielsen, E. B.; Schellman, J. A. *J. Phys. Chem.* **1969**, *8*, 228–243. (b) Nielsen, E. B.; Schellman, J. A. *Biopolymers* **1971**, *10*, 1559–1581. (c) Madison, V.; Schellman, J. A. *Biopolymers* **1972**, *11*, 1041–1076. (d) Rizzo, V.; Schellman, J. A. *Biopolymers* **1984**, *23*, 435–470.

(12) Condon, E. U., Altar, W., Eyring, H. *J. Chem Phys.* **1937**, *5*, 753–775.

(13) (a) Tinoco, I., Jr. *Adv. Chem. Phys.* **1962**, *4*, 113–160. (b) Schellman, J. A. *Acc. Chem. Res.* **1968**, *1*, 144–151.

(14) (a) Kirkwood, J. G. *J. Chem. Phys.* **1937**, *5*, 479–491. (b) Harada, N.; Nakanishi, K. *Circular Dichroic Spectroscopy—Exciton Coupling in Organic Stereochemistry*; Oxford University Press: 1983.

(15) Langgärd, M.; Sandström, J. *J. Chem. Soc., Perkin Trans. 2* **1996**, 435–442.

(16) Sandström, J. In *Circular Dichroism: Interpretation and Applications* Nakanishi, K., Berova, N., and Woody, R. B., Eds.; VCH Publishers: New York, 1994; pp 443–472.

(17) The program is available from Instar Software, IDEON Research Park, S-223 70 Lund, Sweden.

(18) (a) Burkert, U.; Allinger, N. L. *Molecular Mechanics*; ACS Monograph 177, American Chemical Society: Washington, D.C. 1982. (b) The program is available from the Quantum Chemistry Program Exchange (University of Indiana, Bloomington, IN 47405) and from Molecular Design Ltd. (San Leandro, CA 94577).

(9) Koller, H.; Rimböck, K.-M.; Mannschreck, A. *J. Chromatogr.* **1983**, *282*, 89–94.

Table 2. Conformations of Compounds **2** and **3** and Their Energies from MM2(91) Calculations

compd (conformer)	strain energy, kcal mol ⁻¹	C ₆ H ₄ orientation	D _{ac} ^a	bridge orientation ^b
2a	6.29	equatorial	1.19	g ⁻
2b	6.90	equatorial	1.19	g ⁺
2c	7.85	"axial"	1.08	g ⁻
2d	10.84	nearly isoclinal	1.04	g ⁺
3a	8.58	equatorial	1.23	
3b	10.27	pseudoaxial	1.11	

^a According to ref 21. ^b For the (*R*)-configuration.

Results and Discussion

In the previous study⁴ of enantiomer separation and chiroptical properties of *N*-formyl-2-phenyl-1,2,3,4-tetrahydropyridines (**1**) and 14 analogues, the absolute configurations of 11 of the compounds could be assigned by comparison of the experimental CD spectra with theoretical spectra obtained by the matrix method of Schellman and co-workers. Two of these assignments have been corroborated by stereospecific synthesis.¹⁹

The dominant feature in the CD spectra of the 2-aryl compounds and their para substituted derivatives (**1**, Ar = Ph or 4-X-C₆H₄) is a couplet centered at ca. 230 nm, which was assigned to interaction between the $\pi \rightarrow \pi^*$ transition in the *N*-acyl-vinylamine chromophore and the ¹L_a transition in the aromatic chromophore²⁰ by the coupled oscillator mechanism. The latter transition is polarized in the 1–4 direction. The conformational situation in **1** is not quite straightforward. Empirical force-field calculations (MMP2-85)²¹ predicted that the tetrahydropyridine ring has atoms N-1, C-2, C-4, C-5, and C-6 nearly in a plane, while C-3 is outside this plane. Moving C-3 from one side of the ring plane to the other changed the orientation of the 2-substituent from axial to equatorial or vice versa. According to the force-field calculations, the resulting two conformers have rather similar energies. In addition, the acyl group may have the *E* or the *Z* configuration. However, calculations by the Schellman method predicted that all the four possible structures in the *R* configuration should have a negative couplet, which permitted a safe assignment of the absolute configuration.

Empirical force-field calculations on compounds **2** and **3** with MM2-91^{18b} predict the same conformations for the tetrahydropyridine ring as found for compound **1**. The most stable conformations for both compounds has the aryl group in the equatorial orientation (**2a** and **3a**, Table 2). A second conformation of **2** with equatorial aryl group (**2b**) differs from **2a** in the orientation of the tetramethylene bridge. As part of a cyclohexene half-chair the bridge can assume gauche conformations with positive or negative dihedral angles (g⁺ and g⁻, Figure 1). Conformer (*R*)-**2a** is found to have g⁻ and conformer (*R*)-**2b**, g⁺ conformation. The two conformations have rather similar energies (Table 2), and both have to be considered in the analysis of the CD spectrum. Bringing C-3 across the plane of the tetrahydropyridine ring leads to conformers of higher energy (**2c** and **3b**), which can be characterized as axial, although the bridge precludes a distinct axial orientation of the aromatic group. The bridge in (*R*)-**2c** is g⁻. The corresponding conformation with g⁺ (**2d**) has nearly isoclinal groups at C-2. Conformers **2c** and **2d** are so much higher in energy than **2a** that their contributions to the CD spectra can be neglected, and

(19) Ludwig, C. Synthesis of Substituted Piperidines and Pyrrolidines via *N*-Acylimmonium Ions. Ph.D. Thesis, Lund, Sweden, 1992.

(20) Platt, J. R. *J. Chem. Phys.* **1949**, *17*, 484–495.

(21) Liljefors, T.; Tai, J.; Li, S.; Allinger, N. L. *J. Comput. Chem.* **1987**, *8*, 1051–1056.

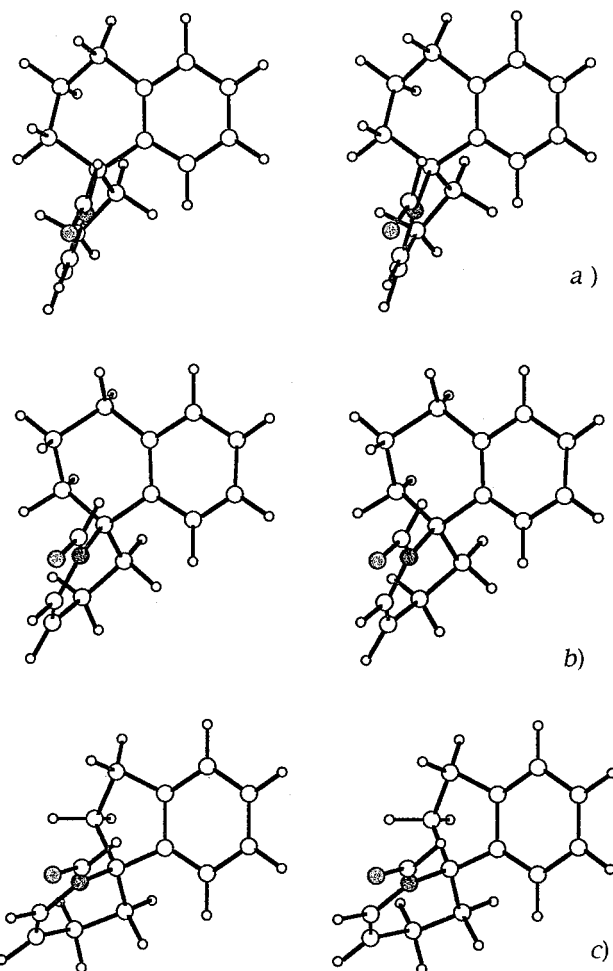


Figure 1. Stereo models of (a) (*R*)-**2a** (g⁻), (b) (*R*)-**2b** (g⁺), and (c) (*S*)-**3a**. The benzene rings are oriented in the same way in all three structures.

the same is true for **3b** with respect to **3a**. The characterization of axial and equatorial substituents is performed as proposed by Anet,²² and the D_{ac} values are given in Table 2.

While the NMR spectra of **1** and its analogues showed the presence of substantial quantities of both *E* and *Z* isomers with respect to the formamido group,⁴ this equilibrium in **2** and **3** is much more biased. The ¹H NMR spectra of both **2** and **3** in CDCl₃ shows *E/Z* ratios of 96:4, corresponding to $\Delta G^\circ = -1.88$ kcal mol⁻¹. In ethanol solution the solvation preferentially occurs through hydrogen bonding to the carbonyl oxygen, which renders the *Z* isomer even more crowded. Therefore, the contribution of the *Z* isomers to the CD spectra can safely be neglected.

Ultraviolet and CD Spectra. The ultraviolet spectra of **2** and **3** are quite similar (Table 3) with a maximum at 242 and 241 nm, respectively (band 1), a shoulder at 210 nm (band 2), and a strong band at 197 nm (band 3). In addition, the spectrum of **3** displays three weaker bands in the range 265–282 nm. Band 1 is assigned to the first $\pi \rightarrow \pi^*$ transition in the *N*-formylvinylamine chromophore. Bands 2 and 3 are assigned to the ¹L_a and ¹B transitions in the benzenoid chromophore²⁰ and the three weak bands in the spectrum of **3** to the ¹L_b transition. The spectrum of the 2-phenyl analogue **1** has a somewhat different appearance with a weak band at 288 nm (¹L_b) and stronger bands at 232 and 204 nm, analogues of bands 1 and 2.

The red-shift of band 1 in going from **1** to **2** and **3** may be due to the orientation of the benzene ring and the more rigid

(22) Anet, F. A. L. *Tetrahedron Lett.* **1990**, *31*, 2125–2126.

Table 3. Ultraviolet and CD^a Spectra of Compounds **1–3** in Ethanol

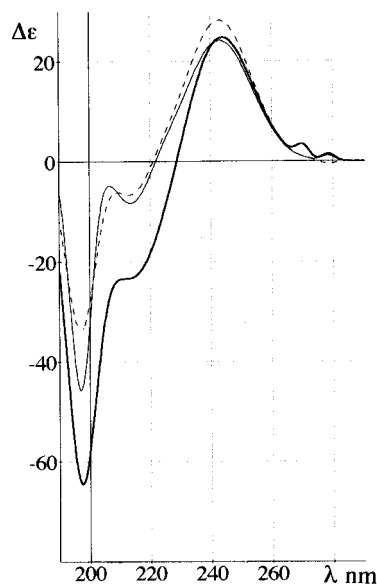
compd	UV/CD	λ_{\max} , nm (ϵ , $\Delta\epsilon$, M ⁻¹ dm ³ cm ⁻¹)
1 ^b	UV	288 (910), 232 (10 200), 204 (14 700)
	CD	257.5 (+1.43), 251 (+11.3), 232 (+10.4), negative end absorption
2	UV	242 (10 200), 210 S ^c (14 900), 197 (47 000)
	CD	279 (+1.39), 270 S (+3.0), 243 (+25.0), 214 (–20), 197 (–65)
3	UV	282 S (1080), 273 (2150), 265 S (3000), 241 (11 100), 210 S (15 400), 197 (40 900)
	CD	277 (–1.33), 270.5 (–1.69), 240 (–14.7), 214 (+11.8), 201 (+30) ^d

^a First eluted enantiomer. ^b From ref 4. ^c Shoulder. ^d End absorption.

Table 4. Experimental^a Rotational Strengths (**R**, in Debye–Bohr Magnetons, $D \cdot \mu_B$) for (+)-**2** and (–)-**3** and Calculated Values for (*R*)-**2** and (*S*)-**3**

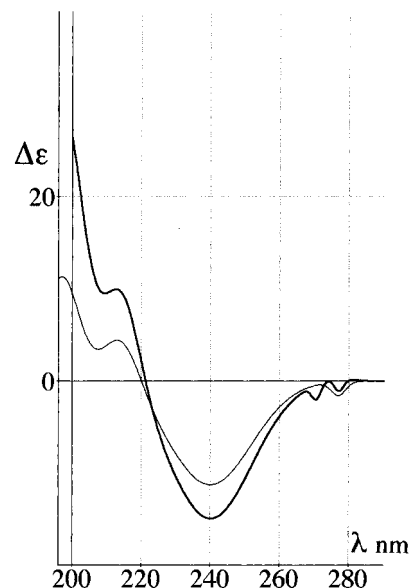
compd	λ , nm	R _{exp}	R _{calc}	
			2a	2b
2	197	–0.856	–0.481	–0.510
	214	–0.774	–0.101	–0.118
	243	+0.696	+0.721	+0.777
	255	–0.064	–0.019	–0.021
	270	+0.017	+0.005 ^c	+0.005
	279	+0.007		
compd	λ , nm	R _{exp}	R _{calc} 3a	
			3a	3a
3	197	+0.662	+0.133	+0.133
	214	+0.217	+0.132	+0.132
	240	–0.452	–0.269	–0.269
	252	–0.078	–0.007	–0.007
	270.5	–0.004	–0.007 ^c	–0.007 ^c
	277	–0.007		

^a Derived by simulating the experimental spectra with gaussians and using eq 1. ^b $1 D \cdot \mu_B = 0.9273 \times 10^{-39}$ cgs units = 3.0917×10^{-53} SI units. ^c Only one ¹L_b transition is included in the calculations.

**Figure 2.** Experimental CD spectrum of (+)-**2** in ethanol (bold full line), and theoretical spectra of (*R*)-**2a** (narrow full line) and (*R*)-**2b** (narrow broken line).

structures of the latter compounds, which permits some homoconjugation between the two chromophores.

The CD spectra of the first eluted enantiomers of **2** and **3** ((+)-**2** and (–)-**3**) show the same transitions as the UV spectra. Weak ¹L_b bands appear at 270 and 279 nm in the spectrum of **2**. The spectra are quite similar although with opposite signs of all bands (Tables 3 and 4 and Figures 2 and 3). Because of strong UV absorption, the spectrum of **3** could only be recorded in the range 290–201 nm, but at shorter wavelengths the intensity increases strongly, and a positive band can be expected in the vicinity of the UV band at 197 nm. The spectra have

**Figure 3.** Experimental CD spectrum of (–)-**3** in ethanol (bold full line), and theoretical spectrum of (*S*)-**3a** (narrow full line).

couplet character, positive for **2** and negative for **3**, indicating interaction by the coupled oscillator mechanism between the first $\pi \rightarrow \pi^*$ transition in the *N*-formylvinylamine chromophore on one side and the benzenoid transitions on the other.

The *N*-formylvinylamine chromophore should also give rise to a $n \rightarrow \pi^*$ transition localized at the carbonyl group, but no band or shoulder corresponding to this transition is observed in the UV or CD spectra of **2** or **3**. Due to the cross conjugation between the vinyl and amide groups the band is expected to fall between ca. 220 nm found for simple amides²³ and 280 nm found for simple ketones. It should be possible to get an idea about the magnitudes, locations, and signs of the $n \rightarrow \pi^*$ CD bands by using the well-known fact that this type of bands undergo much stronger red-shift when going from hydroxylic to nonpolar solvents than $\pi \rightarrow \pi^*$ bands.²⁴ The 243 nm bands of (+)-**2** recorded in ethanol and in a nonpolar solvent (dichloromethane/cyclohexane 1:9, v/v) showed the same intensity, but the band was somewhat broader on the long-wavelength side in the former solvent. The difference spectrum ($\Delta\epsilon_{\text{nonpolar}} - \Delta\epsilon_{\text{EtOH}}$) appears as a negative band with the maximum at 255 nm, $\Delta\epsilon_{\text{max}} = -2.5$ (Figure 4). A similar difference spectrum for (–)-**3** displays a negative band at 252 nm, $\Delta\epsilon_{\text{max}} = -3.0$. These difference spectra should have shown bisignate curves with a positive band at the position of the $n \rightarrow \pi^*$ band in ethanol. Assuming a similar solvent shift as for simple amides, 4000–4500 cm⁻¹,²³ the positive band should fall in the range 225–230 nm. Unfortunately, strong absorption by dichloromethane precludes extension of the difference spectrum to this spectral region, which makes our conclusions somewhat tentative.

(23) Nielsen, E. B.; Schellman, J. A. *J. Phys. Chem.* **1967**, *71*, 2297–2304.

(24) Pimentel, G. C. *J. Am. Chem. Soc.* **1957**, *79*, 3323–3326.

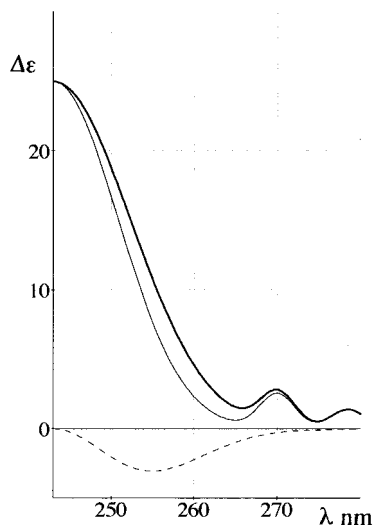


Figure 4. CD spectra of (+)-**2** in ethanol (bold full line) and in dichloromethane/cyclohexane (1:9, v/v) (narrow full line), and difference spectrum (narrow broken line).

In order to assign the absolute configurations of **2** and **3**, calculations by the Schellman matrix method were performed for the low-energy conformations **2a**, **2b**, and **3a**. Because of the substitution pattern, the polarization of the benzenoid transitions in **2** and **3** should be similar to those in *o*-xylene. In this molecule the 1L_b transition is polarized in the direction of the C_2 axis²⁵ and the 1L_a transition is perpendicular to this axis. The 1B transition can be divided into 1B_a and 1B_b components, parallel to the corresponding 1L transitions (Table 1). The UV spectrum of *o*-xylene displays the 1B band at 192 nm ($\epsilon = 53\,000$),²⁶ the 1L_a band at 209.5 nm ($\epsilon = 8600$), and the 1L_b band system at 260 nm ($\epsilon = 260$). Due to the homoconjugation, these bands appear at longer wavelengths and with higher intensities in the spectra of **2** and **3** than in that of *o*-xylene, and the input data are adjusted accordingly (Table 1).

The CD spectrum calculated for the *R* enantiomer of **2**, using the geometry of **2a**, has positive couplet character and shows good agreement with the experimental spectrum for (+)-**2** (Figure 2 and Table 4). All five transitions entered in the calculation come out with correct relative signs and reasonably good intensities. The data calculated with the geometry of **2b** are quite similar, and the assignment of the absolute configuration *R* to (+)-**2** seems well founded. It is worth noting that the calculation for (*R*)-**1**⁴ predicted a negative couplet. The difference is related to the different polarization directions of the benzenoid transitions in **1** and **2**.

The CD spectrum calculated for the *S* enantiomer of **3**, using the geometry of **3a**, shows negative couplet character and generally good agreement with the spectrum of (–)-**3** (Figure 3). The experimental intensities for **3** are considerably lower than for **2** (Table 3), which is reproduced by the calculations (Table 4).

An analysis of the calculations shows that the dominant contribution to $n \rightarrow \pi^*$ rotational strength comes from the one-electron mechanism.

Catalytic asymmetric arylation of 2,3-dihydrofurans with (*R*)-BINAP and Pd(OAc)₂ as catalyst gave large excess of the (*R*)-2-aryl products,¹ and similar results were obtained with *N*-substituted 2,3-pyrroles.² We have now established that the intramolecular arylation⁵ of *N*-formyl-6-(3-{2-[(trifluorometh-

anesulfonyl)oxy]phenyl}propyl)-1,2,3,4-tetrahydropyridine or *N*-formyl-6-[3-(2-iodophenyl)propyl]-1,2,3,4-tetrahydropyridine with the same catalyst gave an enantiomeric excess of (*R*)-(+)-**2**. The corresponding cyclization⁵ of *N*-formyl-6-[2-(2-iodophenyl)ethyl]-1,2,3,4-tetrahydropyridine gave a slight enantiomeric excess of (*R*)-(+)-**3**. However, the difference in activation energy between the routes leading to the (+) and the (–) enantiomer is small for both compounds.

It should be noted that (*S*)-**3** has the same stereochemistry at the quaternary carbon atom as (*R*)-**2**.²⁷ The two compounds have CD spectra with opposite signs for corresponding transitions because the different constraints of the two- and three-carbon bridges lead to quite different relative orientations of the chromophores. The dihedral angles between the transition moments of the $\pi \rightarrow \pi^*$ transition in the *N*-vinylamide chromophore on one side and of the $^1L_a/^1B_a$ and $^1L_b/^1B_b$ transitions on the other with respect to a vector from the midpoint of the benzene ring to the charge-weighted center of the vinylamide chromophore (close to C-2) are +86.6° and +70.1° for (*R*)-**2a** and –71.7° and +73.7° for (*S*)-**3a**. Thus (*R*)-**2a** and (*S*)-**3a** have opposite helicities between the *N*-vinylamide $\pi \rightarrow \pi^*$ transition and the $^1L_a/^1B_a$ transitions and the same helicities with respect to the $^1L_b/^1B_b$ transitions. The dihedral angle for the $^1L_a/^1B_a$ transitions in (*R*)-**2a** is close to 90°, and calculation of the coupling energy V_{12} by the dipole–dipole approximation leads to the prediction that the coupling should be weak. However, in the model used here the interaction occurs between transition charge densities, and inspection of the secular equation reveals that V_{12} is of the same magnitude (74 and 72 cm^{–1}) for the $\pi \rightarrow \pi^* - ^1L_a$ interaction in **2a** and **3a**. The corresponding data for the $\pi \rightarrow \pi^* - ^1B_b$ and $\pi \rightarrow \pi^* - ^1B_a$ interactions are 350 and 106 cm^{–1} for **2a** and 84 and 166 cm^{–1} for **3a**. Thus all three transitions contribute to the negative couplet character of the CD spectrum of (*R*)-**2a**, while the positive couplet character for (*S*)-**3a** can be ascribed to $\pi \rightarrow \pi^* - ^1L_a/^1B_a$ couplings, while the $\pi \rightarrow \pi^* - ^1B_b$ coupling works in the opposite direction. In agreement with this, the CD band near 200 nm is predicted to be twice as intense for (*R*)-**2a** as for (*S*)-**3a**.

Conclusion

We have deduced the absolute configurations of the enantiomers of **2** and **3** by analysis of their CD spectra. According to the assignments given above, (+)-**2** and (+)-**3** both have the *R* configuration and rather similar CD spectra, but they carry the aryl rings on opposite sides of the tetrahydropyridine ring. The result is a caveat against deducing identity in absolute stereochemistry from strong similarity between CD spectra. The need for careful analysis of the transition moments in application of the coupled oscillator mechanism has been stressed by several authors (see e.g. ref 28).

Acknowledgment. We are grateful to the Swedish Natural Science Research Council and the Knut and Alice Wallenberg Foundation for financial support.

JA9635995

(27) This is because the CH₂ groups attached to the spiro atom switch priorities in the Cahn–Ingold–Prelog sequence rules between the two compounds. (a) Cahn, R. S.; Ingold, C. K.; Prelog, V. *Angew. Chem., Int. Ed. Engl.* **1966**, *5*, 385–415 (b) Prelog, V.; Helmchen, G. *Angew. Chem., Int. Ed. Engl.* **1982**, *21*, 567–583.

(28) Hansen, A. E.; Bouman, T. D. *Adv. Chem. Phys.* **1980**, *44*, 545–644, in particular p 595.

(25) (a) Platt, J. R. *J. Chem. Phys.* **1951**, *19*, 263–271. (b) Stephenson, P. E. *J. Chem. Ed.* **1964**, *41*, 234–239.

(26) Jones, L. C., Jr.; Taylor, L. W. *Anal. Chem.* **1955**, *27*, 228–237.